

# Solidification of Quasi-Regular Eutectic

**M. Trepczyńska - Lent**

Faculty of Mechanical Engineering, University of Technology and Life Sciences, Kaliskiego 7 Str.,  
85-796 Bydgoszcz, Poland  
e-mail: address: trema@utp.edu.pl

Received on: 20.04.2007; Approved for printing on: 27.04.2007

## Abstract

The quasi-regular eutectics, one from the groups of the division, accomplished on the basis of the geometry of eutectic phase. The ledeburite eutectic is one from the most commercial eutectics of this group. In the case of rapid solidification, the foundation near which formulate the right growth eutectic they are. One of the measures separating the conditions of low solidification from the rapid one, can be the Peclet number  $Pe$ . Decide to observe solidification eutectic in relationship from the size of the  $Pe$ .

**Keywords:** The theoretical basics of casting processes, Solidification, Eutectic, Peclet number

## 1. Introduction

The examination of a large number of eutectic systems reveals an almost endless variety of microstructures and many attempts have been made to classify the eutectic morphologies on some rational basis, beginning as early as 1922 and 1923. These attempts can be categorized under two general schemes:

- morphological (earlier) classifications,
- interface – type classifications [1].

There are extensive theoretical and experimental studies on the relationship between microstructure and solidification conditions in eutectic growth [2,3,4,5,6].

Besides the above thermal-condition consideration, the eutectic structures are also strongly dependent on the species of the system which can be divided into three groups [7]: (1) lamellar or rod like structure formed in systems in which both phases have low entropies of melting; (2) irregular or complex regular structures formed in systems in which one phase has low entropies of melting and the other has high entropy of melting; (3) special structures formed in the systems in which both phases have high entropies of melting. Based on a lot of experiments,  $\beta$  phases in Al–Si and Sn–Si and other group (2) systems appear in very irregular shape, while the structures are very regular and in

good coupled shape in Sn–Cd,  $CBr_4$ – $C_2Cl_6$  and other group (1) systems [7].

Parameter, influencing the kind of eutectic received, is the fraction of the volume  $g_\alpha$  occupied by one of eutectic phases. Quasi-regular eutectic solidification near the highest value of  $g_\alpha$ , which is over 0,4. They are characterized by lamellar-fibrous morphology.

The typical feature of quasi-regular eutectics, is much about equal volumetric contribution of both eutectic phases and the growth of one of the phases in the shape of the wall crystal. Typical examples of this kind of eutectic can be seen in the Fe–C, Bi–Cd, Sb–Cu<sub>2</sub>Sb and Bi–Au<sub>2</sub>Bi alloys [8].

The characteristic of this group is that although they are in the anomalous (faceted/nonfaceted) class almost regular microstructures can be observed in these eutectics. In the quasi-regular eutectics the high degree of regularity may result from the fact that the faceted phase forms the matrix. Therefore, despite a high entropy of solution value, faceting may be prevented and the unpredicted appearance of almost regular microstructures can be explained [1].

## 2. Theories by Jackson-Hunt and Trivedi

Theoretical and experimental work has been performed to better understand directional solidification of lamellar and rod-like eutectic materials. The distinguished theory of Jackson-Hunt describes steady-state eutectic growth under the following assumptions: (a) lamellar or rod spacing is much smaller than the diffusion distance  $D/V$ , where  $D$  is diffusion coefficient of solute in liquid and  $V$  is the interface velocity, and (b) the interface undercooling is sufficiently small that equilibrium-phase relations apply and the interface composition is approximately the same as the eutectic composition  $C_E$  [9].

A new interpretation of the eutectic growth theory was proposed by Magnin and Trivedi [10]. The effect of the density differences between the eutectic phases is taken into account when calculating the diffusion field. A solution will be derived for non-isothermal interfaces. When the boundary layer composition adjustment is not realized, the growth undercoolings of the two phases become different, and one of the eutectic phases can be overgrown by the other, thus explaining the phenomenon of halo formation observed around the primary graphite particles cast iron. The occurrence of this phenomenon with extremely small composition variations is demonstrated in the transitions from the Fe-Fe<sub>3</sub>C to the stable Fe-C eutectic [10].

Magnin and Trivedi [10] focused on the rapid solidification regime (i.e. large undercoolings and high velocities) and concluded that a model needed that would relax both of the assumptions of the J-H model. Further, they observed: the solution of the growth problem depends on the metastable region of the phase diagram (i.e. undercooled region projected below the equilibrium eutectic temperature), and that a solution was needed for an arbitrary phase diagram. They extended the J-H theory to include rapid solidification conditions, however, they restricted their metastable phase diagram considerations to two specific types and a regular lamellar eutectic morphology. In their first case, the projected values of the liquidus and solidus lines are parallel below the eutectic temperature. Their second case considered an arbitrary redistribution coefficient  $k$ , but was restricted to the case where  $k_\beta = k_\alpha$  [10].

The work [9] recognized that for the important case of asymmetric eutectic phase diagrams, the low volume fraction minority phase was likely to be rod-like, not lamellar. Further, for these asymmetric cases, modest undercooling (low velocity) was sufficient to cause significant differences in metastable phase relations. Consequently, it was undertaken to develop a generalized analytical solution, based on the Jackson-Hunt approach, would: relax both J-H assumptions; address both lamellar and rod-like morphologies; treat an arbitrary metastable phase reaction; and be applicable over the entire parametric range of velocity, interface temperature, and phase relation [9].

## 3. The growth of eutectic phases

Normally in anomalous eutectics, the faceting of one of the phases leads to uncoupled growth and, as a result, a ragged (irregular) solid/liquid interface appears which produces an irregular (divorced) morphology as viewed in a transverse microsection. This is true not only when the volume fraction of the faceted phase is small, but also when it is large, i.e., 40% [1].

Growth of the austenite-iron carbide eutectic (ledeburite) begins with the development of a cementite plate on which an austenite dendrite nucleates and grows (Fig.1). This destabilizes the Fe<sub>3</sub>C, which then grows through the austenite. As a result, two types of eutectic structure develop: a lamellar eutectic with Fe<sub>3</sub>C as a leading phase in the edgewise direction, and rod eutectic in the sidewise direction. Cooling rate significantly influences the morphology of the  $\gamma + \text{Fe}_3\text{C}$  eutectic [11].

Considering more precisely the growth of ledeburite eutectic according to the metastable arrangement, it may be noticed, that after the undercooling bath in relation to the equilibrium temperature of the eutectic transformation, the nucleation of wall phase (Fe<sub>3</sub>C) come into being. They grow up in relation to liquids for the austenite (nonfaceted phase). That in turn, causes with a layer of plates grows in their interdendritic nucleation existence on Fe<sub>3</sub>C plates, and then is changes into planar dendrites. The cementite, which covers planar dendrites spaces in afterwards. The mosaic of alternating plates of both phases is created by the repetition of this process. In consequence austenite shallows are transformed into the fibrous [8].

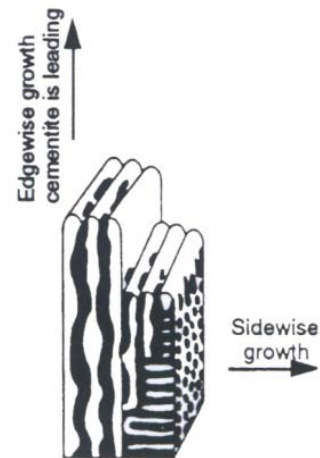


Fig.1. Lamellar and rod growth of the  $\gamma + \text{Fe}_3\text{C}$  eutectic [11]

The growth of cementite eutectic in the eutectic composition cast iron initiates shallow cementite crystallization on the suitable nucleus. In the hypereutectic cementite cast iron it is usually a primitive cementite shallow that solidification. As a result of liquid enrichment by the iron, near the front of the plate crystallization, cementite can crystallize on the plate. The analysis of the kinetics of the eutectic growth shows that nucleation of the austenite is the most probable on the flat part of the plate crystallization. The growth of the austenite nucleus, leads to the planar dendrites creation, closely adjacent to the cementite shallow. In the spaces, between the branches of those dendrites, the liquid is the richest in carbon showing at the same time the largest degree of undercooling in relation to the liquidus line *CD*. This makes possible the growth of cementite in those spaces, growing out of them and creating new cementite cases, between which the austenite grows. The concentration of carbon in the liquid, on the front of the austenite plates, is larger than in the liquid on the front cementite shallow. Such a difference makes possible farther growth of the eutectic with cementite as a leading phase [8].

During the side eutectic growth (*x* direction) the area of undercooling concentration of the liquid solution comes into being that leads to the destabilization of the front, which changes from the planar into cellular one. The growth of the cells leads to carbon enrichment in the intercellular niches, in which cementite can crystallize. Adjacent lamellar cementite shallows join together, the austenite shallow becomes distributed, plate eutectic changes into fibrous eutectic. During the further side growth of eutectic grains only fibrous eutectic still crystallizes.

According to the observations, cementite eutectic changes into either continuous carbides phase with austenite inclusions interpolation of various degree of dispersal, or plate structure that consists of the austenite and cementite plates [12].

Data on the spacing of the ledeburite (Fe+Fe<sub>3</sub>C) in pure Fe-C alloys has been extended to low solidification velocities. The data do not fit the standard theoretical model of  $\lambda^2 V = \text{constant}$ , and it is suggested that this result may be related to the faceted nature of the Fe<sub>3</sub>C component of the ledeburite eutectic [13].

The primary effect of the Si addition on the Fe-Fe<sub>3</sub>C structure of ledeburite is to cause cell and dendrite formation. Both the cells and dendrites of eutectic trough alloys form with plate-shaped cross sections having the rod form of ledeburite growing at right angles to the plane of the plates. The morphologies of the cells and dendrites appear virtually identical to those found in the studies of the pseudobinary eutectic Fe-(Fe,Cr)<sub>3</sub>C [13].

The rod morphology that occurs in the ledeburite structures of Fe-C-Si alloys has a volume percent of the austenite phase of around 43, above the 31,8 % pct maximum value generally thought to be required for rod formation. These experiments confirm that the rod morphology does not form in plane front growth of Fe-C-Si alloys but requires cellular or dendritic formation, where it forms only by growth into the grooves between the cells.

The rod morphology is stabilized because the faceting Fe<sub>3</sub>C matrix phase of the ledeburite is being forced to grow in a specific crystallographic direction, i.e., the direction perpendicular to the plane of cells or dendrites. Limited experimental data indicate this would be the *c* direction of Fe<sub>3</sub>C [13].

Measurements of eutectic interphase spacing  $\lambda$  as a function of growth velocity for Fe-C and Fe<sub>3</sub>C eutectics indicate that growth is occurring at a eutectic spacing. Measured  $\lambda$  was between  $\lambda_{\text{min}} = 2\lambda_0$  and  $\lambda_{\text{max}} = 10\lambda_0$  for Fe-C and  $\lambda_{\text{sr}} = 2\lambda_0$  for Fe<sub>3</sub>C where  $\lambda_0$  is the theoretical value for growth at minimum undercooling [2].

Under slow solidification process, for binary eutectic alloy, once one nucleates first, the other will nucleate dependently on it. Consequently, they grow cooperatively to form lamellar eutectic microstructure. In rapid solidification, the microstructural transition of eutectic alloy, which is from lamellar eutectic to anomalous structure when undercooling increases [14].

The dynamic evolution of the lamellar eutectic of binary alloys in directional solidification has been studied in details using the Monte-Carlo technique [7,15].

## 4. Peclet number

It is understood that  $Pe = (\lambda/2)/(D/V)$  (where *D* is the diffusion coefficient of solute in liquid and *V* is the interface velocity) represents the ratio of spacing to the diffusion length. For a fixed spacing size, a small *Pe* results in a large diffusion length. From the point of view of fluid dynamics, a large diffusion length can deter the rejected solute in front of the interface from diffusing away towards the bulk liquid environment. Thus, the average solute concentration is largely determined by the local solute rejection (partition coefficient) [9].

The Peclet number of concentration is defined with the formula:  $Pe_c = ux/2D$ , where *u* – is the growth velocity, and *x* - depending on the considered phenomenon can be, the length of the wave distortion of the crystallization front, the curvature ray of the dendrite top, interface eutectic distance or the distance between atomic. The number can be one of the measures separating the slow crystallization from rapid crystallization conditions [8].

In the case of rapid crystallization, the foundations according to which the rights of eutectic growth were formulated are unfulfilled. They are related to the necessity of existing considerably smaller interface distance  $\lambda = 2(S_\alpha + S_\beta)$  than the length of diffusion *D/u*, and assuming not big undercooling degree. The composition of liquid little differs then from the eutectic composition *C* on the front of eutectic crystallization  $C(z, 0) \approx C_E$ .

For rapid velocities of the growth, the undercooling degree is large and the interface distance is small in front of very small length of the component diffusion tracts. It is necessary to accept then that the composition of the liquid on the front of crystallization differs from the eutectic composition  $C(z, 0) \neq C_E$ . The Peclet number takes large values in that case.

In the case of fast crystallization the undercooling degree is large, which means that the temperature of the metal drops considerably, and the value of the diffusion coefficient is reduced, because it is connected with the temperature according to the formula:

$$D = D_o \exp(-A/RT) \quad (1)$$

where  $D_o$  he is a constant number,  $A$  - the activation of diffusion energy, and  $R$  - a gas constant.

Accepting the foundation, that the coefficients of the component separation for phases  $\alpha$  and  $\beta$  are equal  $k_\alpha = k_\beta = k_o$  the rights of the plate eutectic growth can be formulated.

After taking into consideration the temperature influence on the diffusion coefficient, it can be noticed that certain maximum speed of eutectic growth exists no matter how big the value of  $k_o$  is. After exceeding such a speed the eutectic growth is little probable. It may be caused by inhibitory influence of the diffusion coefficient or so-called undercooling limit.

For alloys that are characterized by phase equilibrium graphs, for which  $T_o$  line goes near the equilibrium temperature  $T_E$ , for the eutectic transformation, the undercooling limit - that is the difference between the  $T_E$  temperature and the undistribution crystallization temperature - is considerably smaller. When the front of eutectic crystallization reaches the temperature of undistribution eutectic, the Peclet number is larger than one. It means that the distance of the component diffusion  $D/u$  before the single phase is smaller than the diffusion distance required for the coupling growth of the eutectic this  $at$  component before the front of single phase he is  $\lambda/2$ . So now the component  $B$  thrown aside by eutectic phase  $\alpha$  he can not diffusion be transported to second phase  $\beta$  being in the distance  $\lambda/2$  and full coupling growth impossible. He possible is however undistribution the growth of single solid phase, what marks, that  $\lambda \rightarrow \infty$ .

The critical Peclet number  $Pe \approx 1$  exists, above which  $u\lambda^2 \neq const$ , what marks the range rapid crystallization, different rights for which are in force, than in the case of free crystallization [8].

As the Peclet number increases, the diffusion length is reduced. A thinner diffusion layer is favorable for the rejected solute to dissipate into the bulk liquid environment. Therefore, less solute can be accumulated in front of the interface. Consequently, the solute rejection in front of the  $\alpha$  and  $\beta$  phases play equally important roles in determining the average solute concentration. Fig. 3 is an expanded view of Fig. 2 for the low Peclet number regime typical of MnBi/Bi eutectic solidification (low volume fraction and specific  $k$  values) [9].

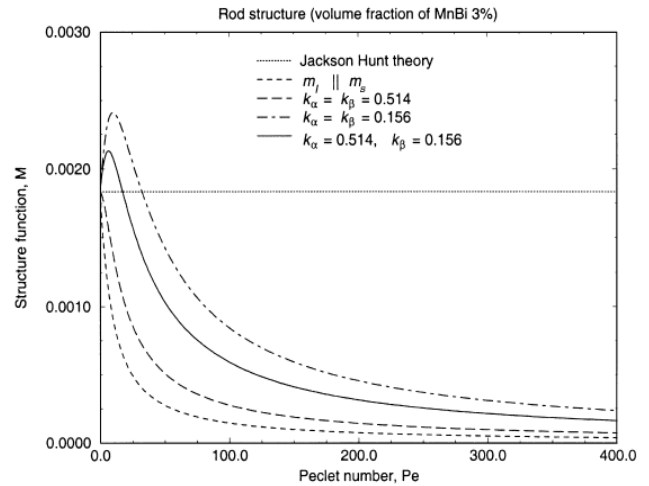


Fig. 2. Rod structure function varying with Peclet number, volume fraction of BiMn is 3% [9]

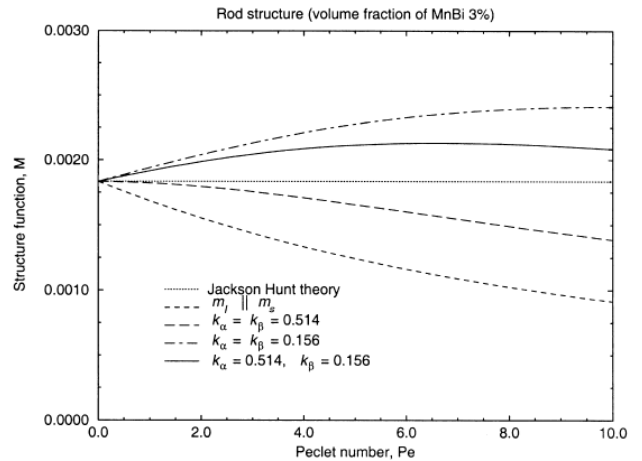


Fig. 3. Rod structure function varying with Peclet number, volume fraction of BiMn is 3% [9]

It should be concluded that for both low Peclet numbers (most crystal growth conditions) and high Peclet number (rapid solidification), the current formulation is preferred if asymmetric (nonequal partition coefficients) phase reactions must be considered [9].

If minimum undercooling is assumed, the Jackson-Hunt theory predicted constant values  $\lambda\Delta T$  and  $\lambda^2V$  for the given volume fraction  $f$ , effective surface energy  $a$ , total rejected solute in front of the  $\alpha$  and  $\beta$  phases  $C_o$ , and the initial solute composition. Trivedi et al. predicted variation in  $\lambda\Delta T$  and  $\lambda^2V$  at high Peclet number conditions for lamellar structures. Applying the current formulation to the MnBi/Bi eutectic growth ( $k_\alpha=0,514$  and  $k_\beta=0,156$ ) was predicted that for a low volume fraction rod structure, that values of  $\lambda\Delta T$  and  $\lambda^2V$  increase significantly as the Peclet number becomes large as shown in Fig. 4. For small Peclet number, the value of  $\lambda\Delta T$  predicted by the current model is almost identical to that obtained by the

Jackson-Hunt theory. However, large values of  $\lambda\Delta T$  are predicted by the current formulation using the phase reaction of MnBi/Bi and Trivedi-like phase relations with constant partition coefficients of 0,514 and 0,156 respectively [9]. The solutions of  $\lambda\Delta T$  with a phase reaction of Trivedi II bracket exact solution at high Peclet number which is consistent with authors [10] for the lamellar structure [9].

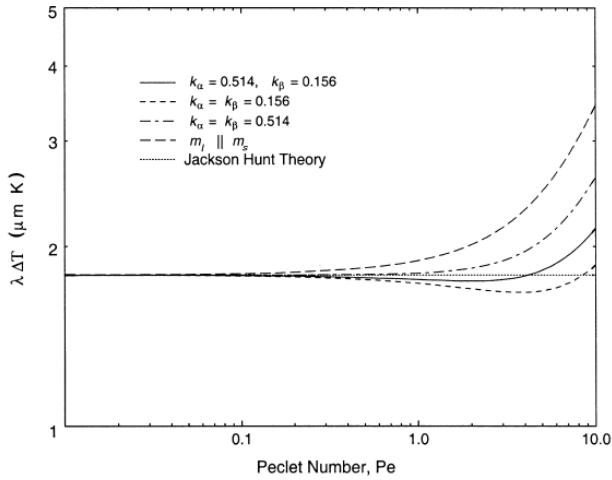


Fig. 4. Dependence of  $\lambda\Delta T$  on Peclet number  $Pe$  [9]

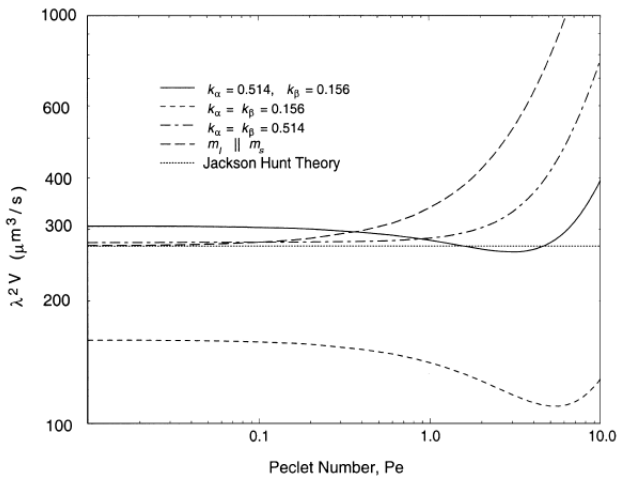


Fig. 5. Dependence of  $\lambda^2 V$  on Peclet number  $Pe$  [9]

Fig. 5. displays the dependence of  $\lambda^2 V$  on Peclet number predicted by the Jackson–Hunt theory, and the current formulation based upon phase reactions of Trivedi’s with MnBi/Bi values. At moderate or high  $Pe$  number, the  $\lambda^2 V$  increase as the partition coefficient increases for the given Peclet number so that the predictions using Trivedi’s phase diagram bracket the exact solution. At a fairly low Peclet number, the value of  $\lambda^2 V$  depends not only on the individual partition coefficient for each phase, but also the difference between the two phases, e.g.  $(k_\beta - k_\alpha)$ , indicating that the correlation of spacing and growth velocity is complex. For each solution, however, the  $\lambda^2 V$  relationship appear constant over the low Peclet number regime.

For the eutectic growth of BiMn/Bi, the average eutectic spacing is at the micro level, and high growth velocity is at the order of the magnitude of 10 cm/h. This leads to the Peclet number of 0,034, in a region of most crystal growth conditions [9].

At usual growth rates ( $V \approx 0,1$  to  $1000 \mu\text{m/s}$ ), the Peclet number is of the order of  $10^{-3}$  to  $10^{-1}$ . Under these conditions, the difference between the exact value and the approximation of  $\omega_n$  (“frequency” factor) is smaller than 1% , and therefore negligible when compared to the precision with which the physical constants of the alloy are known. The effect, due to large undercoolings, of the temperature dependence of the diffusion coefficient and of the liquidus and solidus compositions has been neglected. As a rule of thumb, one can consider that the calculations are valid for growth up to a few cm/s [10].

Figure 6 is a schematic diagram of a lamellar eutectic structure which forms under steady-state directional solidification conditions,  $f_\alpha, f_\beta$  the relative phase amount [16].

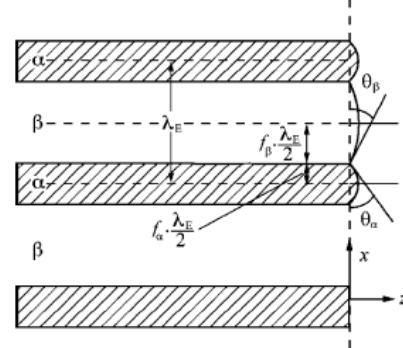


Fig. 6. A schematic diagram of a lamellar structure [16]

The undercooling at the eutectic interface is obtained as:

$$\lambda_E \Delta T_E = K_2 \left( 1 + \frac{P}{P + \lambda_E \frac{\partial P}{\partial \lambda_E}} \right) \quad (2)$$

with

$$P(f_\alpha, Pe, k_\alpha, k_\beta, C_\infty) = \frac{1}{Pe \Delta C_\infty} \sum_{n=1}^{\infty} \left[ B_n \frac{\sin(n\pi f_\alpha)}{n\pi} \right] \quad (3)$$

For  $k_\alpha = 0,999999$  and  $k_\beta = 10^{-6}$  the variation in the  $P$ -function with  $f_\alpha$  for different  $Pe$  is shown in Fig. 7a and the variation in the  $P$ -function with  $Pe$  for different  $f_\alpha$  is shown in Fig. 7b. The corresponding  $k_\alpha = k_\beta \rightarrow 1$  can be found in Fig. 9a i 9b in [17] and for  $k_\alpha = k_\beta \rightarrow 1$  in Fig. 8a i 8b [17]. For a symmetrical case ( $k_\alpha = k_\beta = k$ ) and small  $Pe$  the variation in the  $P$ -function with  $f_\alpha$  is independent of  $k$  and equal to the  $P$ -function of the Jackson-Hunt approach [17]. This curve is also shown in Fig. 7a (bold black). The comparison shows that for  $k_\alpha \neq k_\beta$  the  $P$ -function becomes unsymmetrical with respect to  $f_\alpha$  even for small  $Pe$ . Therefore, it is generally not described by the J-H model. For the symmetrical case with small  $k$  the  $P$ -function increases with increasing  $Pe$  (Fig. 9b in [17]), for large  $k$  the  $P$ -function decreases with increasing  $Pe$  (Fig. 8b in [17]).

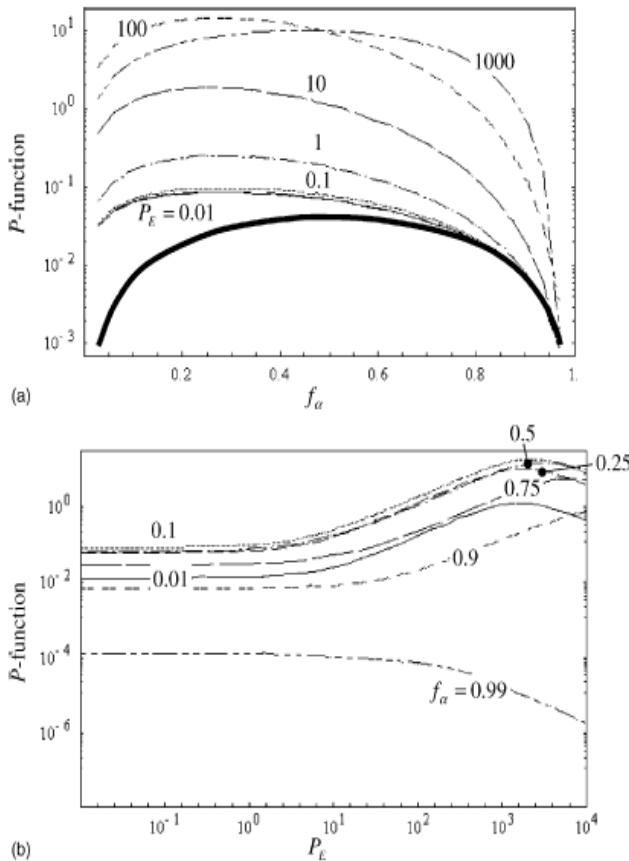


Fig. 7. The variation in the  $P$ -function: (a) with  $f_\alpha$  for different values of  $Pe$  and (b) with  $Pe$  for different values of  $f_\alpha$ . The distribution coefficients were chosen extremely different with  $k_\alpha = 10^{-6}$  and  $k_\beta = 0,999999$ .  $C_\infty$  was set to 0,5. The bold black curve in (a) represents the prediction of the Jackson–Hunt model [16]

As shown in Fig. 7, in the unsymmetrical case the  $P$ -function increases with increasing  $Pe$  for most value of  $f_\alpha$ , only for  $f_\alpha = 0,99$  it decreases. From that finding it is obvious that in the unsymmetrical case, the smaller of the two distribution coefficients dominates the eutectic process. In the present case ( $k_\alpha = 0,9999999$ ;  $k_\beta = 10^{-6}$ ) the  $\alpha$ -lamellae grow without any significant solute redistribution. On the other hand, the solute redistribution ahead of the  $\beta$ -lamellae is large and further growth of these lamellae can only occur if diffusion reduces the high solute concentration in front of the lamella. Therefore, diffusion of the element with the smaller  $k$  is more important than diffusion of the other species [16].

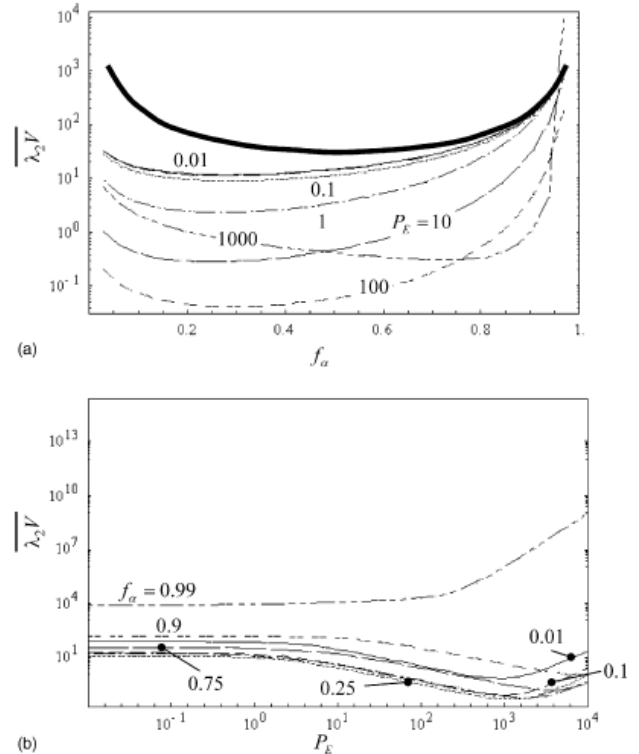


Fig. 8. The variation in  $\lambda_E^2 V$ : (a) with  $f_\alpha$  for different values of  $Pe$ , and (b) with  $Pe$  for different values of  $f_\alpha$ . The distribution coefficients were chosen extremely different with  $k_\alpha = 10^{-6}$  and  $k_\beta = 0,999999$ .  $C_\infty$  was set to 0,5. The bold black curve in (a) represents the prediction of the Jackson–Hunt model [16,17]

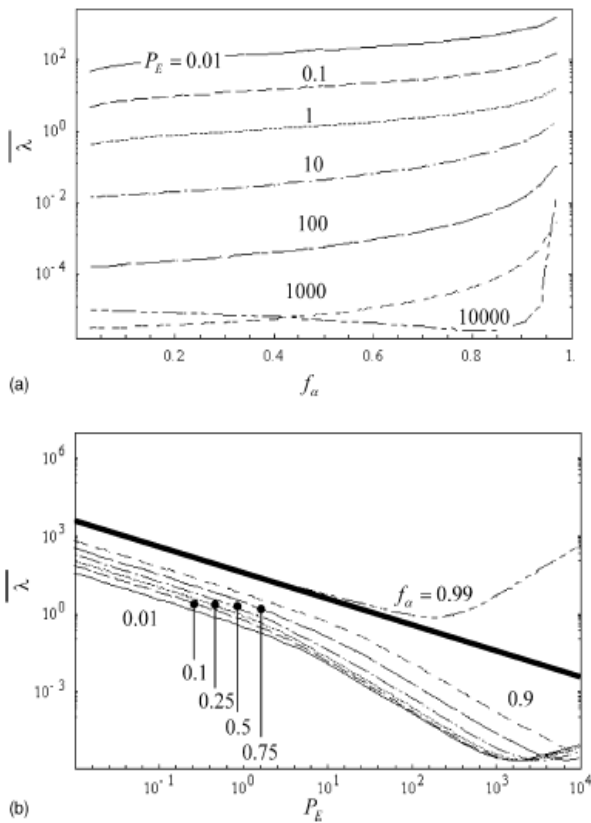


Fig. 9. The variation in  $\lambda_E$ : (a) with  $f_a$  for different values of  $Pe$ , and (b) with  $Pe$  for different values of  $f_a$ . The distribution coefficients were chosen extremely different with  $k_a = 10^{-6}$  and  $k_b = 0,999999$ .  $C_\infty$  was set to 0,5. The bold black curve in (b) represents the prediction of the Jackson–Hunt model for  $f_a = 0,99$  [16,17]

## 5. Conclusions

Solidification of quasi-regular eutectic has been analyzed many times. No one of unambiguous theory that describes relationship between lamellar spacing and the growth rate has been created so far.

The eutectic solidification is a complex issue connected with the Peclet number value. This work is only a trial of viewing the present knowledge of the quasi-regular eutectic solidification, which leads to the conclusion of necessity of carrying in-depth research.

## References

- [1] M.A. Savas, R.W. Smith, Quasi-regular growth: a study of the solidification of some high volume-fraction faceted phase anomalous eutectics, *Journal of Crystal Growth* 71 (1985) 66-74.
- [2] H. Jones; W. Kurz, Relation of interphase spacing and growth temperature to growth velocity in Fe-C and Fe-Fe<sub>3</sub>C eutectic alloys, *Zeitschrift fuer Metallkunde*, v 72, n 11, Nov (1981) 792-797.
- [3] E. Fraś, M. Górný, H. Lopez, Gradient structure of ductile iron, *Archiwum Odlewnictwa R.* 6 nr 18 (2/2) (2006) 39-44 (in Polish).
- [4] E. Fraś, M. Górný, Relationship between undercooling and eutectic cell count in cast iron, *Archiwum Odlewnictwa R.* 6 nr 21 (1/2) (2006) 377-382 (in Polish).
- [5] E. Guzik, D. Kopyciński, The casted eutectic {Al-Fe} composite {it in situ}, *Archiwum Odlewnictwa R.* 2 nr 4 (2002) 347-352 (in Polish).
- [6] P. Magnin, W. Kurz, An analytical model of irregular eutectic growth and its application to Fe-C, *Acta Metall.* vol. 5, 35 (1987) 1119-1128.
- [7] W.M. Wang, X.P. Hu, S.F. Zhang, X.F. Bian, J.M. Liu, Effect of element bonding energy on the microstructure in the growth of eutectic alloys, *Computational Materials Science* 29 (2004) 214-220.
- [8] E. Fraś, *Crystallization of metals*, WNT, Warsaw, 2003 (in Polish).
- [9] L.L. Zheng, D. J. Larson Jr., H. Zhang, Revised form of Jackson-Hunt theory: application to directional solidification of MnBi/Bi eutectics, *Journal of Crystal Growth* 209 (2000) 110-121.
- [10] P. Magnin, R. Trivedi, Eutectic growth: a modification of the Jackson-Hunt theory, *Acta Metall. Mater.* Vol. 39, No 4 (1991) 453-467.
- [11] L. Nastac, D.M. Stefanescu, Prediction of gray to white transition in cast iron by solidification modeling, *AFS Transactions* (1195) 329-337.
- [12] Cz. Podzucki, *Cast iron. Structure, properties, application*, ZG STOP, Cracow, 1991 (in Polish).
- [13] J. S. Park, J. D. Verhoeven, Directional solidification of white cast iron, *Metallurgical and Materials Transactions A*, Vol. 27A (1996) 2328-2337.

- [14] W.J. Yao, N. Wang, B. Wei, Containerless rapid solidification of highly undercooled Co-Si eutectic alloys, *Material Science and Engineering A* 344 (2003) 10-19.
- [15] W.M. Wang, Y.C. Niu, S.F. Zhang, X.F. Bian, J.M. Liu, Effect of cluster deposition on the eutectic structure in binary systems: A Monte-Carlo simulation, *Journal of Alloys and Compounds* 407 (2006) 215-220.
- [16] A. Ludwig, S. Leibbrandt, Generalised Jackson-Hunt model for eutectic solidification at low and large Peclet numbers and any binary eutectic phase diagram, *Material Science and Engineering A* 375-375 (2004) 540-546.
- [17] R. Trivedi, P. Magnin, W. Kurz, Theory of eutectic growth under rapid solidification conditions, *Acta Metall.* 35 (1987) 971-980.